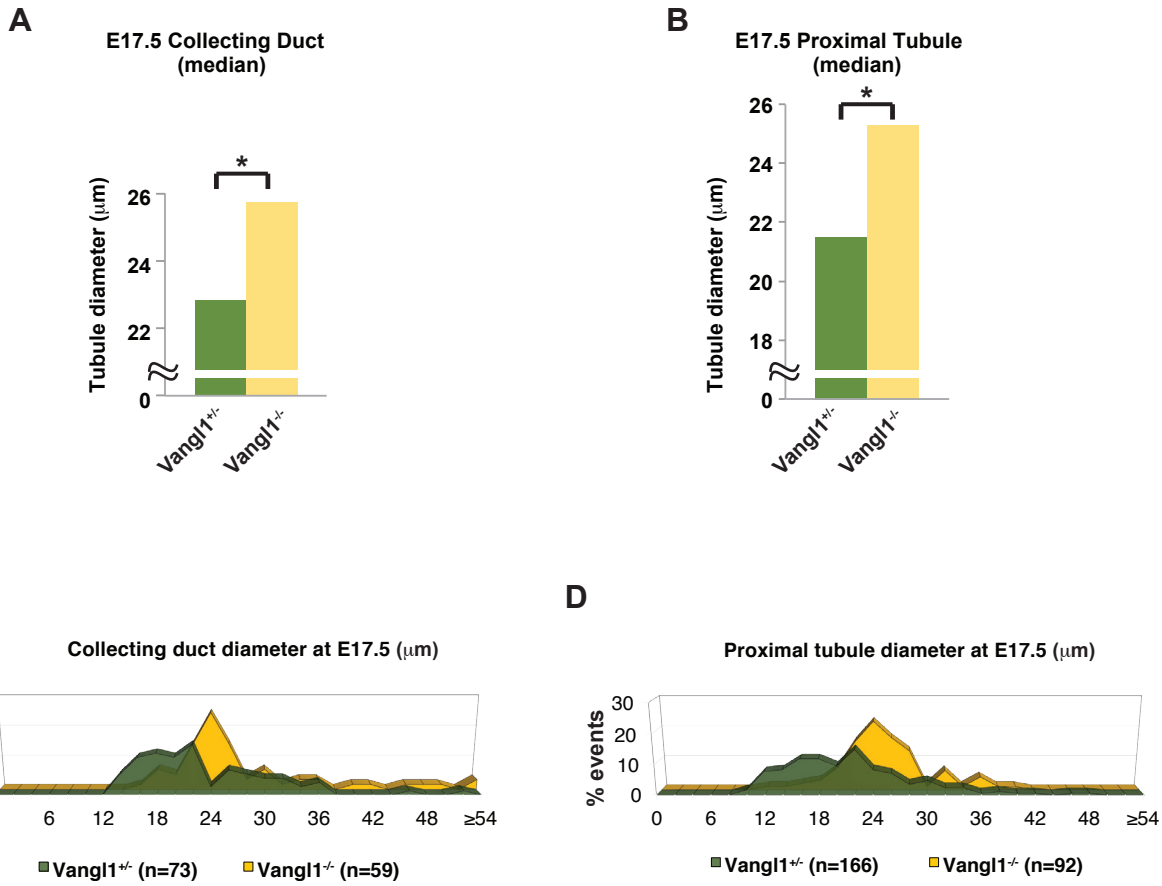
A
E17.5 Collecting Duct
(median)
Tubule diameter (μm)
26
24
22
0
*
Vangl1+/-
Vangl1-/-
B
E17.5 Proximal Tubule
(median)
Tubule diameter (μm)
26
24
22
20
18
0
*
Vangl1+/-
Vangl1-/-
C
Collecting duct diameter at E17.5 (μm)
% events
30
20
10
0
0
6
12
18
24
30
36
42
48
≥54
Vangl1+/- (n=73)
Vangl1-/- (n=59)
D
Proximal tubule diameter at E17.5 (μm)
% events
30
20
10
0
0
6
12
18
24
30
36
42
48
≥54
Vangl1+/- (n=166)
Vangl1-/- (n=92)

Figure S1. Vangl1 mutant tubule diameters are enlarged at E17.5. Related to Figure 1.

Median collecting duct (A) and proximal tubule (B) diameters in control (*Vangl1*$^{+/-}$) and *Vangl1*$^{-/-}$ mutant kidneys. (C-D) Distribution of diameters from (A) and (B), respectively. Measurements made using the low calcium dehydration method.

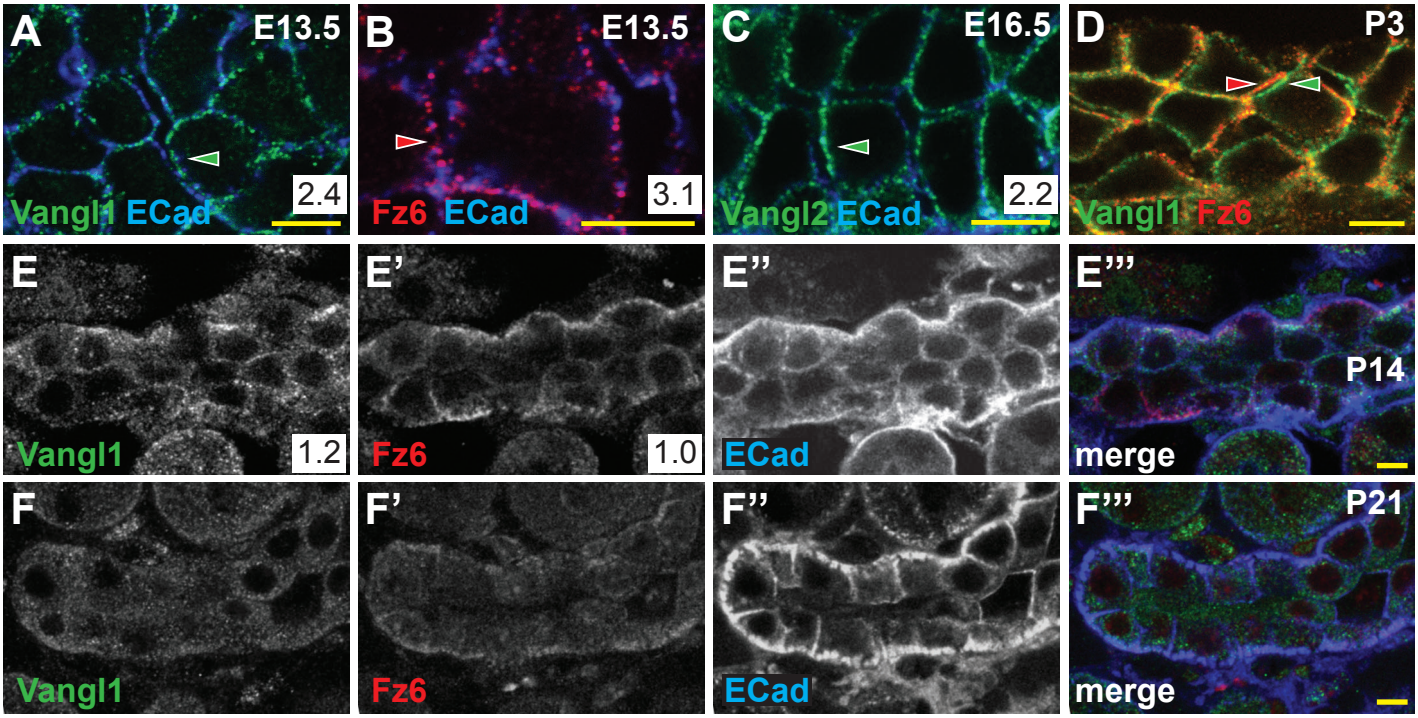
A
E13.5
Vangl1 ECad
2.4
B
E13.5
Fz6 ECad
3.1
C
E16.5
Vangl2 ECad
2.2
D
P3
Vangl1 Fz6
E
Vangl1
1.2
E'
Fz6
1.0
E''
ECad
E'''
P14
merge
F
Vangl1
F'
Fz6
F''
ECad
F'''
P21
merge

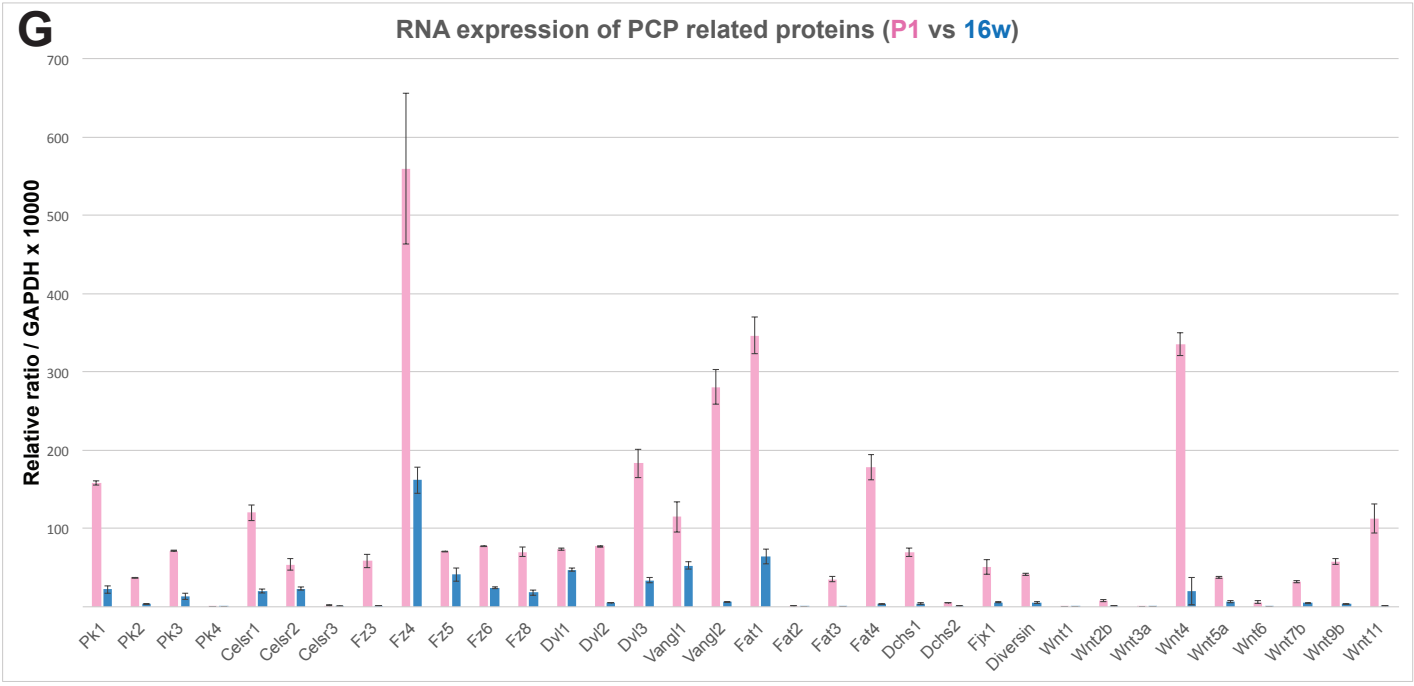
G
RNA expression of PCP related proteins (P1 vs 16w)
Relative ratio / GAPDH x 10000
700
600
500
400
300
200
100
Pk1
Pk2
Pk3
Pk4
Celsr1
Celsr2
Celsr3
Fz3
Fz4
Fz5
Fz6
Fz8
Dvl1
Dvl2
Dvl3
Vangl1
Vangl2
Fat1
Fat2
Fat3
Fat4
Dchs1
Dchs2
Fjx1
Diversin
Wnt1
Wnt2b
Wnt3a
Wnt4
Wnt5a
Wnt6
Wnt7b
Wnt9b
Wnt11

Figure S2. Embryonic PCP protein asymmetric localization and expression declines postnatally. Related to Figure 2. (A-F) Collecting ducts from WT kidneys stained for Vangl1 (green) or Fz6 (red) and E-Cadherin (blue) from age E13.5 to P21. Asymmetric Vangl1 and Fz6 localization are seen throughout embryonic stages and through P3. Membrane associated staining of PCP proteins declines after P3, with some residual membrane associated signal and mostly cytoplasmic signal evident at P15. By P21, minimal membrane associated signal remains. See also Figure 7 for comparable P30 images. (G) qPCR of PCP and related genes, normalized to GAPDH, at P1 and 16 weeks shows decreased gene expression over this time span. Scale bars: 5 μm.

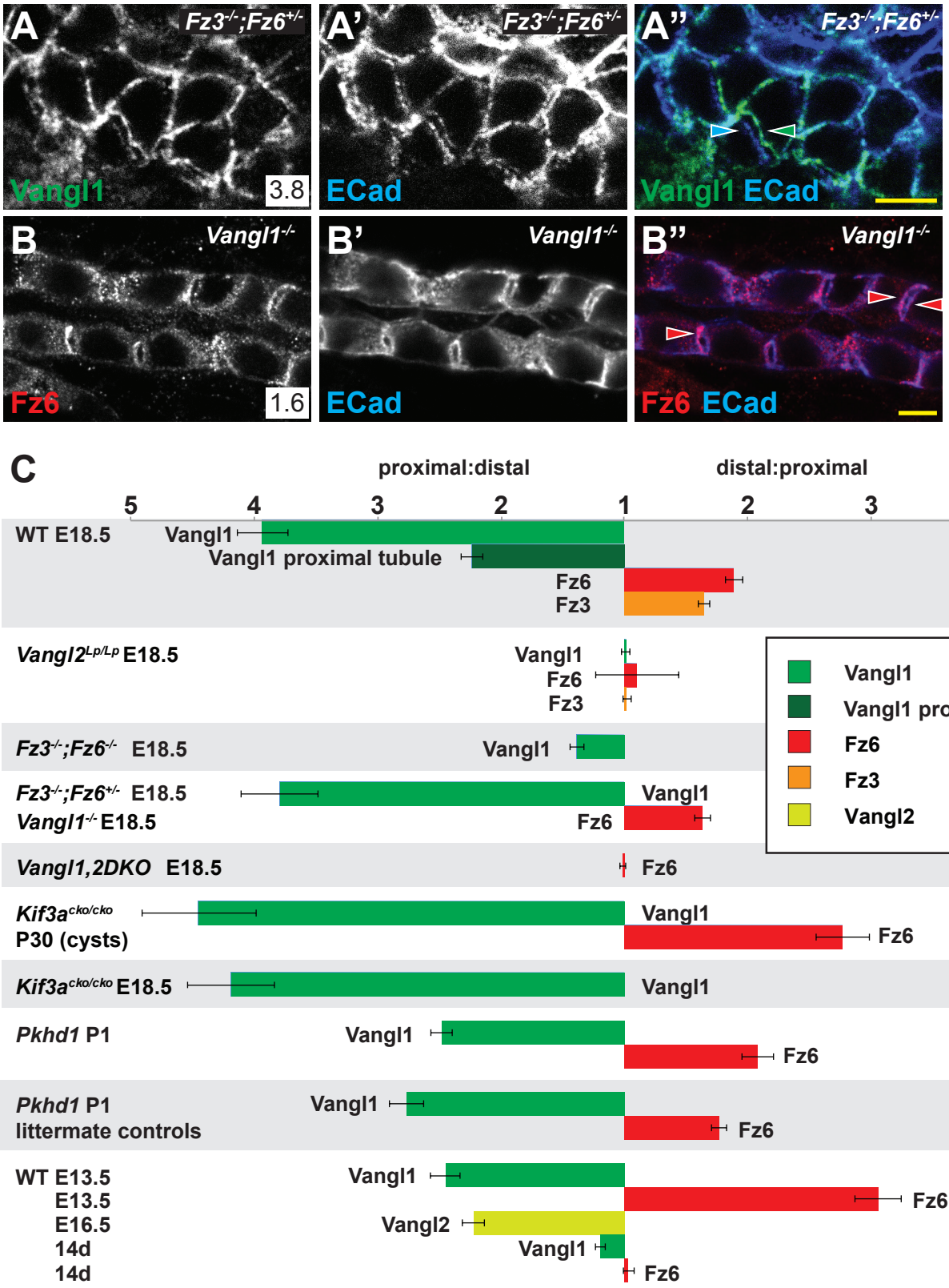
A
Fz3-/-;Fz6+/-
Vangl1
3.8
A'
Fz3-/-;Fz6+/-
ECad
A''
Fz3-/-;Fz6+/-
Vangl1 ECad
B
Vangl1-/-
Fz6
1.6
B'
Vangl1-/-
ECad
B''
Vangl1-/-
Fz6 ECad
C
proximal:distal
distal:proximal
5
4
3
2
1
2
3
4
WT E18.5
Vangl1
Vangl1 proximal tubule
Fz6
Fz3
Vangl2Lp/Lp E18.5
Vangl1
Fz6
Fz3
Fz3-/-;Fz6-/- E18.5
Vangl1
Fz3-/-;Fz6+/- E18.5
Vangl1-/- E18.5
Vangl1
Fz6
Vangl1,2DKO E18.5
Fz6
Kif3acko/cko
P30 (cysts)
Vangl1
Fz6
Kif3acko/cko E18.5
Vangl1
Pkhd1 P1
Vangl1
Fz6
Pkhd1 P1
littermate controls
Vangl1
Fz6
WT E13.5
E13.5
E16.5
14d
14d
Vangl1
Fz6
Vangl2
Vangl1
Fz6
Vangl1
Vangl1 prox
Fz6
Fz3
Vangl2

Figure S3. Asymmetric localization of core PCP protein localization in E18.5 PCP mutants. Related to Figure 3. (A-A'') Vangl1 (green) and E-Cadherin (blue) in *Fz3*$^{-/-}$*; Fz6*$^{+/-}$ kidneys. One copy of Fz6 is sufficient to support PCP signaling as assessed by Vangl1 asymmetric localization. (B-B'') Fz6 (red) and E-Cadherin (blue) in a *Vangl1*$^{-/-}$ mutant collecting duct. Asymmetric localization of Fz6 is modestly diminished though not lost. Scale bars: 5 μm. (C) Graph of Intensity Ratios (IRs) representing asymmetry of core PCP protein distributions for conditions examined throughout the manuscript. All values are for collecting ducts unless marked otherwise. Ratios are shown ± SEM. See STAR Methods for method of measurement.

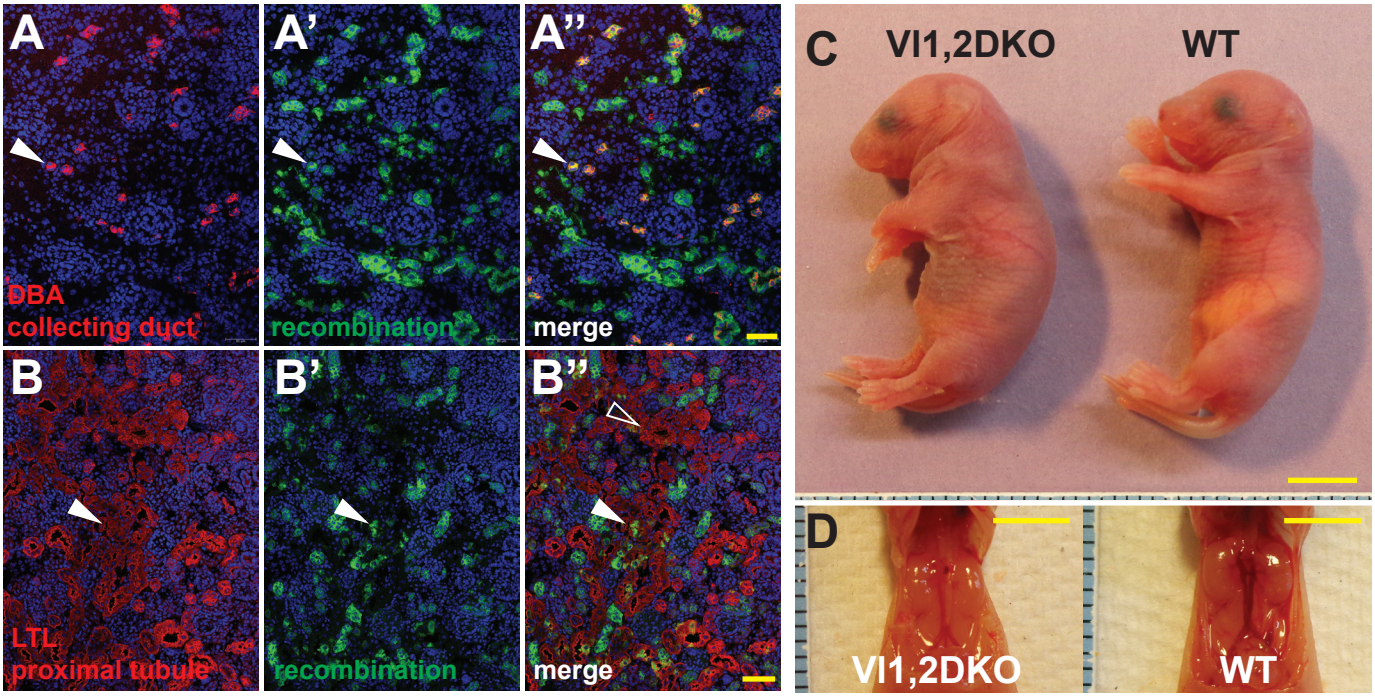

Low calcium dehydration method

E Collecting duct diameter at E18.5 (μm)

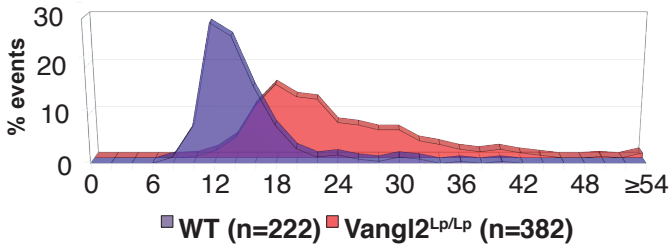

F Proximal tubule diameter at E18.5 (μm)

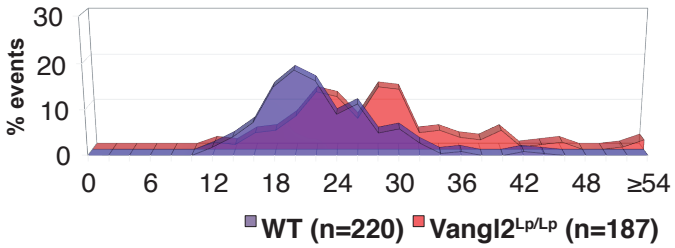

Standard fixation method

G Collecting duct diameter at E18.5 (μm)

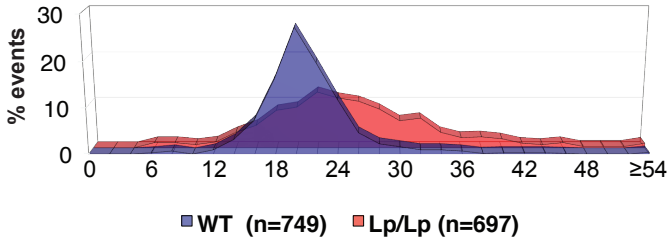

H Proximal tubules diameter at E18.5 (μm)

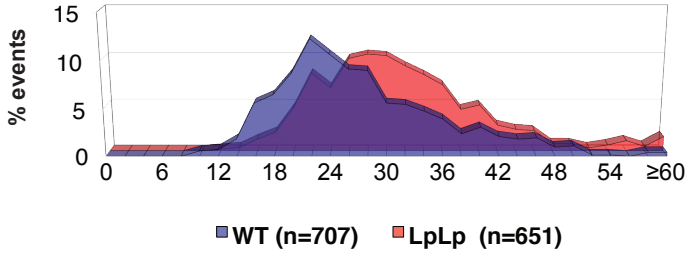

Figure S4. Validation of the Vangl1,2 DKO mutant kidneys. Related to Figure 4. The mTmG reporter [S1] in P1 Vl1,2DKO kidneys stained for AQP2 (A-A''; red; collecting duct) or LTL (B-B''; red; proximal tubules) and DAPI (blue) showing only the GFP (green) signal from mTmG indicating recombination. Virtually all collecting duct cells display recombination, and a small number of proximal tubule cells show recombination. (C-D) Gross views of VL1,2DKO and control mice and kidneys. (E-H) Comparison of the low calcium dehydration fixation and standard fixation for measurement of tubule diameters. Low calcium dehydration fixation data (E-F) are from Figure 1 J and K, respectively. The same relationships, but with different absolute values, are observed. Scale bars: A",B", 50 μm; C,D, 5 mm.

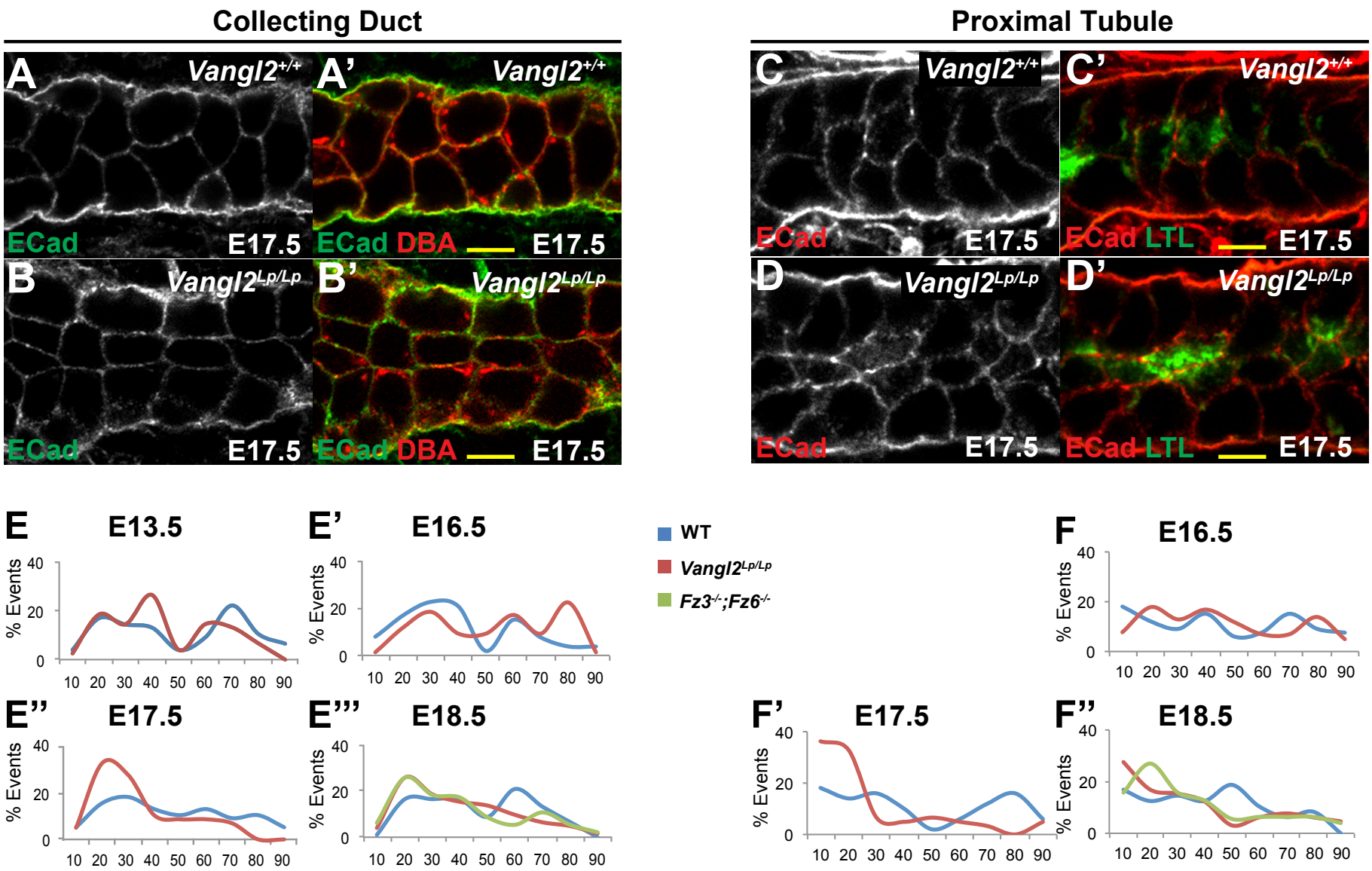
Collecting Duct
Proximal Tubule
A
Vangl2+/+
ECad
E17.5
A'
Vangl2+/+
ECad DBA
E17.5
B
Vangl2Lp/Lp
ECad
E17.5
B'
Vangl2Lp/Lp
ECad DBA
E17.5
C
Vangl2+/+
ECad
E17.5
C'
Vangl2+/+
ECad LTL
E17.5
D
Vangl2Lp/Lp
ECad
E17.5
D'
Vangl2Lp/Lp
ECad LTL
E17.5
E
E13.5
E'
E16.5
E''
E17.5
E'''
E18.5
WT
Vangl2Lp/Lp
Fz3-/-;Fz6-/-
F
E16.5
F'
E17.5
F''
E18.5
% Events
0
20
40
10 20 30 40 50 60 70 80 90
Degrees from Tubule Axis

Figure S5. Cell shapes suggesting CE in E17.5 collecting duct and proximal tubule. Related to Figure 5. (A-B') WT control or *Vangl2*$^{Lp/Lp}$ collecting ducts stained for E-Cadherin (green) and DBA (red) to illustrate altered cell shape and orientation in the mutant. (C-D') WT control or *Vangl2*$^{Lp/Lp}$ proximal tubules stained for E-Cadherin (red) and LTL (green) to illustrate altered cell shape and orientation in the mutant. (E-E''') Plots of orientation of cellular long axes relative to the tubule axis for WT control, *Vangl2*$^{Lp/Lp}$ and *Fz3*$^{-/-}$*; Fz6*$^{-/-}$ collecting ducts from E13.5 to E18.5. (F-F''') Plots of orientation of cellular long axes relative to the tubule axis for WT control, *Vangl2*$^{Lp/Lp}$ and *Fz3*$^{-/-}$*; Fz6*$^{-/-}$ proximal tubules from E16.5 to E18.5. We speculate that the biphasic distribution of wild type orientations may result from rosette configurations through which cells were shown to transition in *Xenopus* [S2]. Regardless, a shift toward the long axis is consistent with CE. Scale bars: 5 μm.

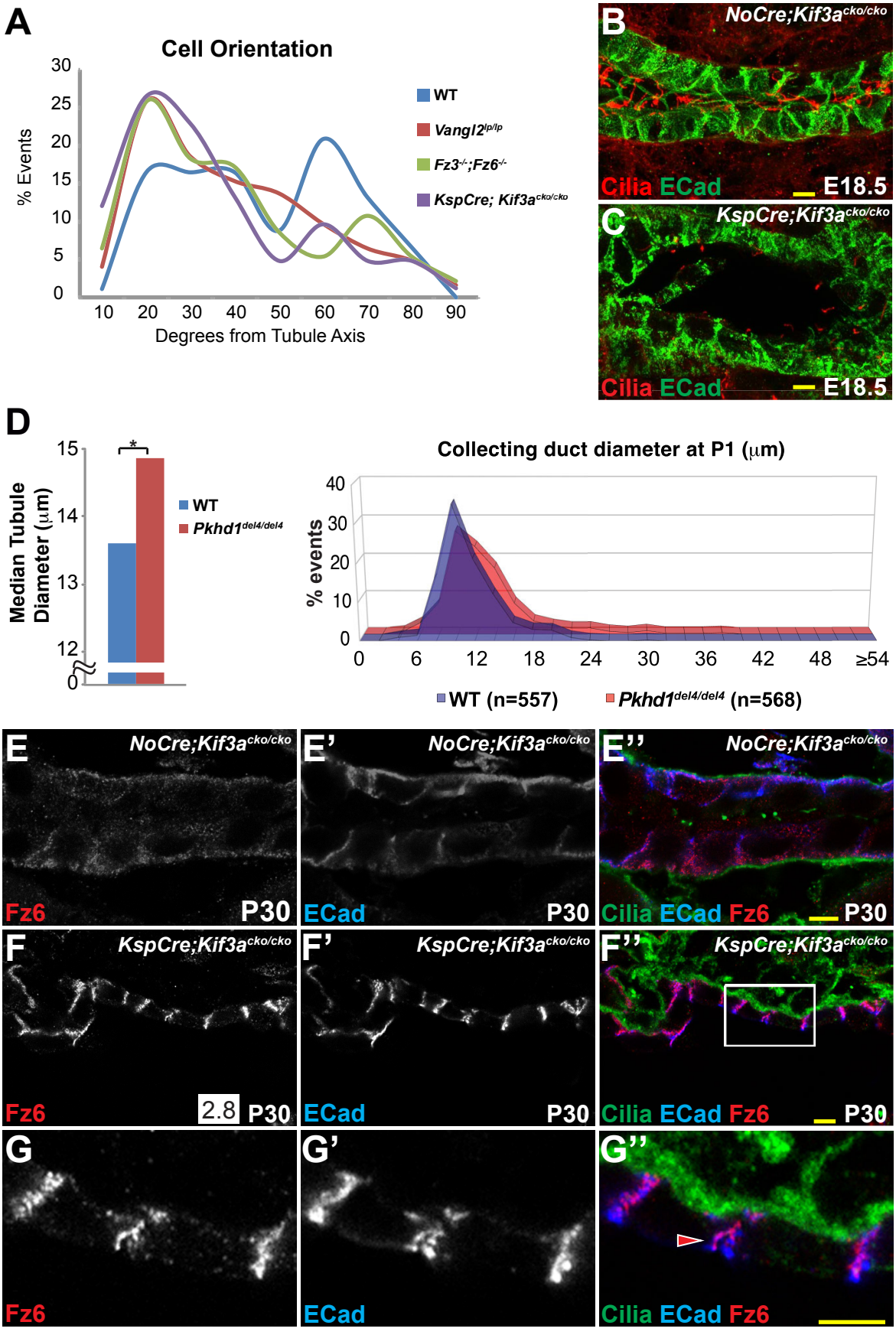
A
Cell Orientation
% Events
30
25
20
15
10
5
0
10 20 30 40 50 60 70 80 90
Degrees from Tubule Axis
WT
Vangl2lp/lp
Fz3-/-;Fz6-/-
KspCre; Kif3acko/cko
B
NoCre;Kif3acko/cko
Cilia ECad
E18.5
C
KspCre;Kif3acko/cko
Cilia ECad
E18.5
D
Median Tubule Diameter (μm)
15
14
13
12
0
*
WT
Pkhd1del4/del4
Collecting duct diameter at P1 (μm)
% events
40
30
20
10
0
0 6 12 18 24 30 36 42 48 ≥54
WT (n=557)
Pkhd1del4/del4 (n=568)
E
NoCre;Kif3acko/cko
Fz6
P30
E'
NoCre;Kif3acko/cko
ECad
P30
E''
NoCre;Kif3acko/cko
Cilia ECad Fz6
P30
F
KspCre;Kif3acko/cko
Fz6
2.8
P30
F'
KspCre;Kif3acko/cko
ECad
P30
F''
KspCre;Kif3acko/cko
Cilia ECad Fz6
P30
G
Fz6
G'
ECad
G''
Cilia ECad Fz6

Figure S6. Analysis of Kif3a mutant precystic and cystic kidneys. Related to Figure 6. (A) Plots of orientation of cellular long axes relative to the tubule axis for E18.5 *KspCre;Kif3a*$^{cko/cko}$ collecting ducts plotted with data for WT control, *Vangl2*$^{Lp/Lp}$ and *Fz3*$^{-/-}$*; Fz6*$^{-/-}$ collecting ducts from Figure S5E'''. (B-C) WT control (*NoCre;Kif3a*$^{cko/cko}$) and *KspCre;Kif3a*$^{cko/cko}$ collecting ducts stained at E18.5 for acetylated-α-tubulin (red; cilia) and E-Cadherin (green) showing residual short cilia in the mutant ducts. (D-D''') E18.5 *KspCre;Kif3a*$^{cko/cko}$ collecting duct stained for Vangl1 (green), E-Cadherin (blue), acetylated-α-tubulin (red; cilia) and DBA (white; collecting duct), showing asymmetric Vangl1 localization in precystic mutant. (E-E'') WT control (*NoCre;Kif3a*$^{cko/cko}$) and (F-F'') *KspCre;Kif3a*$^{cko/cko}$ kidneys stained at P30 for Fz6 (red), E-Cadherin (blue) acetylated-α-tubulin (green; cilia). Low levels of mostly cytoplasmic Fz6 and E-Cadherin (overexposed in E-E'') remain in the WT control collecting ducts. Fz6 and E-Cadherin are strongly expressed in the *KspCre;Kif3a*$^{cko/cko}$ cysts. (G-G'') Higher magnification image of a *KspCre;Kif3a*$^{cko/cko}$ mutant cyst (boxed region of F) stained for Fz6 (red) and E-Cadherin (blue) showing asymmetric localization of Fz6 at a cell-cell junction that separated during fixation. Scale bars: 5 μm.

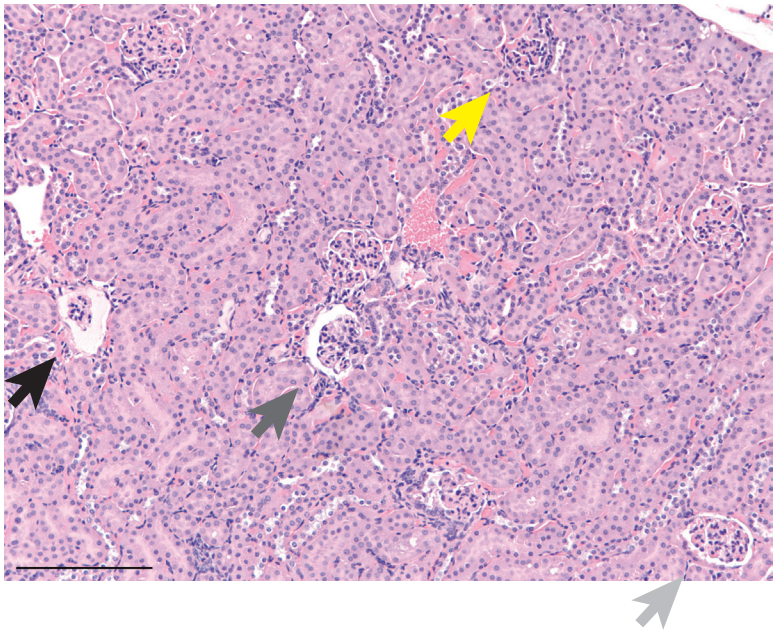

Figure S7. Vl1,2DKO kidney showing the GCKD phenotype. Related to Figure 7. 16w H&E stained kidney showing glomeruli with dilated capsules varying in severity (grey to black arrows) and one nearly normal glomerulus (yellow arrow). Scale bar: 200 μm.

age (weeks)	number of animals	animals with GCKD phenotype/ no. examined
3	1	0/1
16	10	1/9
24	1	
29	1	
32	1	
35	1	0/1
50	1	1/1

Table S1. Vangl1,2 DKO mice examined for cysts. Related to Figure 4.

gene name	primer, sense	primer, antisense
GAPDH	GACTTCAACAGCAACTCCCAC	TCCACCACCCTGTTGCTGTA
Pk1	GATGGAGAAAGCAAGCCAAG	TGTGCAGCATGGAAGAGTTC
Pk2	ACATGGGCACTCTCAACTCC	TGTATCCTAGGGGGTTGCTG
Pk3	TGCTGTTTCGAGTGTGAAGC	CATCACAGTATTCCGCATGG
Pk4	CCACAGGACAGTGATGAACG	CCTTCAAGCTTAGGAGGCAG
Celsr1	ATGCTGTTGGTCAGCATGTC	GGGATCTGGACAACAACCG
Celsr2	GCTGTGTGTGAGCATCTCGT	CATCATGAGTGTGCTGGTGT
Celsr3	GGAGTTGAAAGAGGCAAGGA	CTTCTCAGAGCCAGGGAGG
Fzd3	GAATCAGGTCTGGACGACTCA	CATCTGGGAGACAACATGGA
Fzd4	TGGCACATAAACCGAACAAA	TACAACGTGACCAAGATGCC
Fzd5	GGATGATTAGGGCTCCGACT	CCGCCACAGGTACCTAGCTT
Fzd6	AAAAGCTTGGCAAAGGAACA	ATTATGACCAGGGGATCGCT
Fzd8	CGGTTGTGCTGCTCATAGAA	CAGTCATCAAGCAGCAAGGA
Dvl1	GGCAACTTGGCATTGTCATC	GGTGCACGCCTACAAATTCT
Dvl2	ACACAAGCCAGGAGACAACC	TCCATGGATCAGGATTTTGG
Dvl3	CAGGGTAGCTTGGCATTGTC	GCGGCCCAGCTATAAGTTCT
Vangl1	GATGCTGTTAGGAGGTTCGG	AGTCCCGCTTCTACAGCTTG
Vangl2	TGCTGGACAAGTGGGCTTAT	GTGCGCTGCGGATACAAA
Fat1	ATTCCAAGCGACTCGAGAAA	GAGGCAAGTTTGGAGCTACG
Fat2	ACCAGCTTGGACACTTCACC	CAGCCACTTCTGTGTCCTCA
Fat3	TCACGGGAACAAACTGTGAA	CACACTCGTCCACATCATCC
Fat4	TCCGTCAGAGTGGTGTCAAG	GTTGGCCACAATGATGACAG
Dachsous1	AGTGGAACAACCACCTCTGG	GGCCTAGAGCAGTGTGGGTA
Dachsous2	TCAGCGGCAACTTACACAAC	GGTCAGACGCAAGAATCACA
Fjx1	TCTTCGGATCCAATCTCCAC	GTTCTGGAAGGGCAAACTCA
Diversin	TTGTGAGGCCCAAGGATAAG	TCCAGTCTGCTGATCACACC
Wnt1	TAGTCGCAGGTGCAGGACTC	CTCTTCGGCAAGATCGTCA
Wnt2b	TGTCTGGGTAGCGTTGACAC	CTGCTGCTGCTACTCCTGACT
Wnt3a	GGTGGCTTTGTCCAGAACAG	ACTACGTGGAGATCATGCCC
Wnt4	TCTGGATCAGGCCTTTGAGT	CCTGCGACTCCTCGTCTTC
Wnt5a	CCGGGCTTAATATTCCAATG	ACGCTTCGCTTGAATTCCT
Wnt6	CCTGCAGATGCTGGTAGGAT	CGGTAGAGCTCTCAGGATGC
Wnt7b	CTCCCCGATCACAATGATG	GCGTCCTCTACGTGAAGCTC
Wnt9b	GGAAGGGTGTCAGGACCTC	CGAGGAGATGCGAGAGTGC
Wnt11	AGGCCCTCCAGCTGTTTAC	GTCTGCGAGGCTCTGCTCT

Table S2. Primers for qPCR. Related to STAR Methods.

Supplemental References

S1. Muzumdar, M.D., Tasic, B., Miyamichi, K., Li, L., and Luo, L. (2007). A global double-fluorescent Cre reporter mouse. Genesis *45*, 593-605.

S2. Lienkamp, S.S., Liu, K., Karner, C.M., Carroll, T.J., Ronneberger, O., Wallingford, J.B., and Walz, G. (2012). Vertebrate kidney tubules elongate using a planar cell polarity-dependent, rosette-based mechanism of convergent extension. Nat Genet *44*, 1382-1387.